# Control Approach Of A Grid Connected Dfig Based Wind Turbine Using Mppt And Pi Controller

*Samatar ABDI YONIS*[1], *Ziyodulla YUSUPOV*[1], *Adib HABBAL*[2] *Olimjon TOIROV*[3]

[1]Department of Electrical and Electronics Engineering, Institute of Graduate Programs, Karabuk University, Street No: 7, 78050 Karabuk, Turkey
[2]Department of Computer Engineering, Institute of Graduate Programs, Karabuk University, Street No: 7, 78050 Karabuk, Turkey
[3]Department of Electrical Machines, Power Engineering Faculty, Tashkent State Technical University named after Islam Karimov, University Street 2, Tashkent city, Uzbekistan

saamabdi4f@gmail.com, ziyadullayusupov@karabuk.edu.tr, adibhabbal@karabuk.edu.tr, olimjontoirov@gmail.com

DOI: 10.15598/aeee.v21i3.5149

Article history: Received Mar 29, 2023; Revised Aug 5, 2023; Accepted Aug 28, 2023; Published Sep 30, 2023.


***Abstract.*** *A double-fed induction generator (DFIG) has been frequently utilized in wind turbines due to its ability to handle variable-speed operations. This study investigates the real parameters of the Mitsubishi MWT 92/2.4 MW wind turbine model. It performs and implements grid-connected variable-speed turbines to control the active and reactive powers. Moreover, it presents a vector control strategy for DFIG for controlling the generated stator power. The unique feature of the approach proposed in the study is the comparison between two control techniques - the Maximum Power Point Tracking (MPPT) algorithm and the Proportional-Integral (PI) controller - for regulating DFIG based wind turbine systems. Thus, the result demonstrates that the performance of the MPPT technique provides strong robustness and reaches steady-state much faster than the PI controller with variable parameters. To the contrary, a typical PI controller gives a fast response when tracking the references of DFIG magnitudes. The effectiveness of the overall system is tested by MATLAB simulation.*

## Keywords

***DFIG, PI controller, MPPT algorithm, vector control, wind turbine.***

## 1. Introduction. Problem Definition

Wind energy is a popular renewable source of energy, and its use is increasing steadily across the world. Wind technology is promoted in several nations through different government programs and market mechanisms. An alarming advancement have been observed in the wind power system across the world in the last decades with increasing rotor diameters and utilization of advanced power electronics that operate at a variable speed [1]. In comparison to other forms of wind power system, DFIG is found to be the most extensively /studied machine. The study in [2] demonstrates an overview of grid-connected wind energy conversion system (WECS) in details. Precise detection of the grid voltage angle has been noted to be an essential task in most of the control techniques in the GSC [2] and [3]. Furthermore, it has been recommended that all advanced wind turbines must include a faster and efficient tracking equipment to determine the frequency and stator voltage of DFIG during the grid synchronization.

The study in [3] provides a review on the issue of effective estimations of wind speed (EEWS). The main EEWS strategies and their implementations are thoroughly addressed. The study demonstarted that an accurate estimations of the wind speed is important for energy capture. Improving the effectiveness of vector control (VC) strategy has attracted many researchers.

In several studies [4], [5], [6], and [7], the authors presented that wind turbine-based DFIG provides decouple control of active or reactive power of the system, resulting in good dynamic performance, higher efficient energy output, and good power quality. Recall that DFIG is more difficult to control compared to the typical induction generator. Hence, the rotor currents are regulated by the power electronics converter in the rotor circuit, which results in the control of DFIG [8]. VC is a popular strategy for controlling DFIG-based wind turbines [9] and [10]. The technique presented in [11] introduces a new integrated frequency control technique that dynamically integrates inertial and pitch angle control to enhance the performance of DFIG in power system frequency control. Different studies have been conducted investigating DFIG control; for instance, a novel controller has been introduced that allows the DFIG system to positively contribute to grid operation [12]. Further, a comparative analysis between robust sliding mode control (SMC) and typical PI controller in DFIG based WECS has been presented [13]. Their simulated results demonstrate that the proposed SMC provides a faster response with very little steady state error in comparison with the PI. Moreover, comparing PI and fuzzy control based DFIG wind turbine, it is obvious that fuzzy control is more robust against machine parametric perturbations and delivers faster convergence [14]. According to the study in [15], by using a fuzzy-PI controller, the settling time and the value of peak overshoot have reduced, and variations are damped down faster compared with the typical PI controller. Besides, the transient response given by fuzzy-PI controller has also proven to be better than typical PI controllers. The study in [16] introduces a dual-loop control technique to enhance the dynamic performance of DFIG that may be subjected to grid disturbance. This technique can quickly deteriorate the fluctuations of stator flux and successfully mitigate the impact of stator transient flux on the performance of the DFIG. Further, in [17] the comparative investigations of control strategies have been considered in DFIG system. It states that direct torque control (DTC) is quicker than VC in terms of transient response, that can be very beneficial and provide a lot of capacity when specific control manipulations are required. The research in [18] investigates a coordinated control approach for DFIG with a DC connection. The experimental findings suggest that a control approach is available for the proposed power grid configuration. It concludes that the DC/DC converter is the most important component in WECS for the integration of the DFIG system. From [19], it can be realized that the study places a PI controller before the conventional DTC or direct power control (DPC) blocks to improve the dynamic performance. Consequently, the study shows that DTC has higher operating performance than DPC since DTC directly controls the torque.

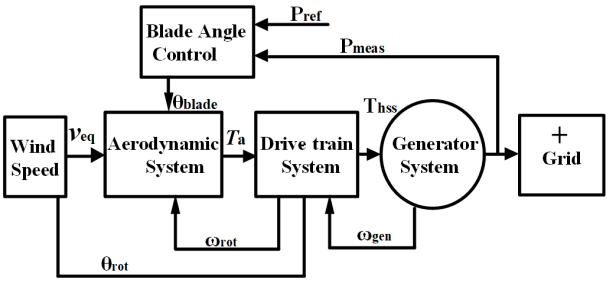


**Fig. 1:** Typical block diagram of wind turbine system.

Numerous control techniques for DFIG, such as DPC, VC approach, and DTC, have been suggested throughout the years [20]. The VC strategy has advantages among other control techniques; for example, it gives reduced harmonic distortion and fewer power ripples [1], [10], and [21]. However, VC has been applied only for PI control strategy in the literature [22] and [23]. But, in our study PI controller and MPPT techniques has been performed. Moreover, none of the aforementioned literature analyzes the performance and control of the magnitudes of grid-connected DFIG system using PI and MPPT controller in terms of settling time. Here, the DC-link capacitor is used to separate RSC and GSC. The DC link stores the energy in the capacitor and the purpose of this capacitor is to keep the voltage terminals constant.

This study assesses the real parameters of the Mitsubishi MWT 92/2.4 MW wind turbine model integrated with a grid connected DFIG system using the VC strategy. This study is organized into several sections. Section I briefly presents the overview of the wind turbine-based DFIG system. Wind turbine modeling has been developed in Section 2. . The VC strategy of both sides - RSC and GSC are given in Section 3. . Two types of control method schemes - PI controller and MPPT for DFIG have been demonstrated in Section 4. . The simulation result has been discussed in Section 5. , and finally, conclusions are drawn which are stated in Section 6. .

## 2. Wind Turbine Model

Normally, wind turbines generate electricity by converting mechanical energy provided by the kinetic energy of the wind [21]. Here, the wind turbine model comprises several parts: a wind speed, an aerodynamic system, a mechanical or drive train system, and a generator. A typical block diagram of a wind turbine is given in Fig. 1.

## 2.1. Wind Speed Model

Wind speed tends to vary depending on the nature of the environment and it fluctuates randomly over time. This explains the fact that it has a significant impact on the electromagnetic torque and hence it seems to have a major impact on the power generated by the three blades [24]. Thus, to simulate the dynamic performance of wind turbine model, the wind speed should be taken into consideration. In this work, wind speed can be modeled by adding the following four constituents:

$$v_w(t) = v_{wa}(t) + v_{wt}(t) + v_{wr}(t) + v_{wg}(t), \quad (1)$$

where $v_{wa}(t)$, $v_{wr}(t)$, $v_{wg}(t)$ and $v_{wt}(t)$ are the constant, turbulence, ramp, and gust constituents, respectively. The gust constituent can be modeled to represent unusual transient increases in wind speed and can be formulated as follows:

$$v_{wg}(t) = \begin{cases} 0 & , \text{for} : t < T_{sg} \\ A_g\left(1 - \cos\left[2\pi\left(\dfrac{t - T_{sg}}{T_{eg} - T_{sg}}\right)\right]\right) & , \text{for} : T_{sg} \leqslant t \leqslant T_{eg} \\ 0 & , \text{for} : T_{eg} < t \end{cases}, \quad (2)$$

where $T_{sg}$ and $T_{eg}$ are start and end time of gust constituents and $A_g$ is gust amplitude. Eventually, the turbulence constituent can be indicated by a signal with the following power density [24].

$$P_{Dt}(f) = \frac{l v_w \left[\ln\left(\frac{h}{z_0}\right)\right]^2}{\left[1 + 1.5\frac{fl}{v_w}\right]^{5/3}}, \quad (3)$$

where $l$ is turbulence scale, $h$ is the height and $l = 20h$, that has maximum height of 300 meter; $z_0$ is the raggedness length value for different landscape type as it can be seen in Tab. 1 [24].

**Tab. 1:** Values of $z_o$ for various landscape type [24].

| Types of landscape | Scale of $z_o$ in (meter) |
|---|---|
| High seas | 0.001-0.01 |
| Snow surface | 0.01-0.05 |
| Mown grass | 0.01-0.03 |
| Rocky ground | 0.02-0.1 |
| Mountainous | 2-6 |

Since we know all the other values, the next stage is to generate a signal with power spectrum. Considering that the $P_{Dt}$ is close to the responses of first-order filter, then the suggested transfer function is as follows:

$$H(s) = \frac{K}{s + p}, \quad (4)$$

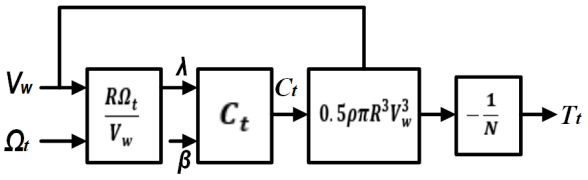


**Fig. 2:** Aerodynamic system of wind turbine.

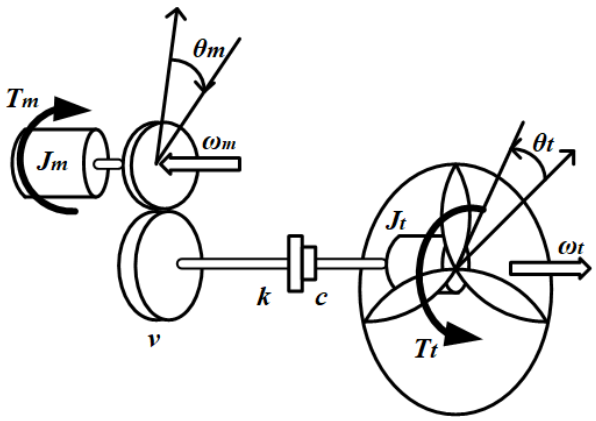


**Fig. 3:** Drive train system of wind turbine.

Where $p$ and $K$ are formulated as follows:

$$p = \frac{2\pi\left(\left(K_1^2\right)^{3/5} - 1\right)}{K_2\sqrt{K_1^2 - 1}}, \quad (5)$$

$$K = K_1 p, \quad (6)$$

And $K_1$ and $K_2$ are expressed as:

$$K_1 = l v_w \left[\ln\left(\frac{h}{z_0}\right)\right]^{-2}, \quad (7)$$

$$K_2 = 1.5\frac{1}{v_w}. \quad (8)$$

The calculated signal of the power spectrum is defined as:

$$P_{filter} = \frac{\frac{k^2}{p^2}}{1 + \frac{4\pi^2}{p^2 f^2}}. \quad (9)$$

## 2.2. Aerodynamic Model

Normally, the aerodynamic system of a wind turbine calculates the electromagnetic torque as shown in Fig. 2 and is given as [20].

$$T_t = 0.5\rho\pi R^3 V_w^2 C_t, \quad (10)$$

Where, $\rho$, $R$, $V_w$, and $C_t$ are air density, radius (meter), wind speed and torque coefficient of wind turbine, respectively.

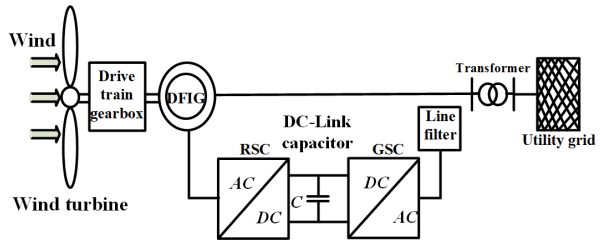


**Fig. 4:** The proposed power circuit.

The power coefficient is given as:

$$C_p = 0.77\left(\frac{151}{\lambda_i} - 0.58\beta - \frac{1}{500}\beta^{2.14} - \frac{26.4}{2}\right)\left(e^{-18.4/\lambda_i}\right), \tag{11}$$

with

$$\lambda_i = \frac{1}{\lambda + 0.02\beta} - \frac{0.003}{\beta^3 + 1}. \tag{12}$$

The tip step ratio can be obtained as:

$$\lambda = \frac{R\Omega_t}{V_w}. \tag{13}$$

## 2.3. Drive Train System

In some literature [25] it is possible to model the drive train system in a 2-mass where the stiffness of the shaft links the rotor of DFIG to the turbine mass as it can be seen in Fig. 3. Drive train contains of a turbine, low-speed shaft, generator, gearbox, and high-speed shaft [26] and [27].

For instance, the torque ($T_m$) and stator reactive power ($Q_s$), can be formulated as follows:

$$T_m = \frac{3}{2}PM\left(i_{sq}i_{rd} - i_{sd}i_{rq}\right), \tag{14}$$

and

$$Q_s = \frac{3}{2}PM\left(v_{sq}i_{sd} - v_{sd}i_{sq}\right), \tag{15}$$

Where: $\theta_t$, $\theta_m$, $\omega_t$ and $\omega_m$ are turbine angle, generator angle, turbine and generator angular speed, respectively; $\tau_t$ is torque supplied to rotor shaft, and $\tau_m$ is generator torque; $P$ is number of poles; $M$ is magnetizing inductance.

## 2.4. Generator Model

For a proper understanding of the behaviors of a generator or DFIG system, it is important to use a basic and special model such as rotating 2-phase $dq$ which is provided by Park transform technique [28]. Fig. 4 represents the power circuit of DFIG. The dynamic equation of the system is given as a fourth order state space based synchronous $dq$ representation, stator and rotor voltage equations can be given [22]:

$$\begin{aligned} v_{ds} &= r_s i_{ds} + \frac{d\psi_{ds}}{dt} - \omega_s\psi_{qs}, \\ v_{qs} &= r_s i_{qs} + \frac{d\psi_{qs}}{dt} + \omega_s\psi_{ds}, \\ v_{dr} &= r_r i_{dr} + \frac{d\psi_{dr}}{dt} - \omega_r\psi_{qr}, \\ v_{qr} &= r_r i_{qr} + \frac{d\psi_{qr}}{dt} + \omega_r\psi_{dr}. \end{aligned} \tag{16}$$

The stator and rotor fluxes are determined:

$$\begin{cases} \psi_{ds} = L_s i_{ds} + L_m i_{dr}, \\ \psi_{qs} = L_s i_{qs} + L_m i_{qr}, \\ \psi_{dr} = L_r i_{dr} + L_m i_{ds}, \\ \psi_{qr} = L_r i_{qr} + L_m i_{qs}. \end{cases} \tag{17}$$

Stator active and reactive powers are given:

$$\begin{cases} P_s = \frac{3}{2}\left(v_{ds}i_{ds} + v_{qs}i_{qs}\right) \\ Q_s = \frac{3}{2}\left(v_{qs}i_{ds} - v_{ds}i_{qs}\right) \end{cases} \tag{18}$$

# 3. Vector Control Strategy

Controlling alternating current (AC) machines may be generally categorized into two, namely scalar and vector controls. The implementation of scalar control is simple and may produce an approximate steady state response, especially when the dynamics are slow. For this purpose, to achieve a higher accuracy and better dynamics and also good response during steady state, VC strategies have to be applied [23]. The VC strategy focuses on RSC and GSC control.

## 3.1. Rotor Side Converter Control

The main idea behind the control of RSC is to keep rotational speed constant regardless of wind speed. The rotor voltage can be defined as:

$$v_{dr} = r_r i_{dr} + \sigma L_r\frac{di_{dr}}{dt} - \omega_r\sigma L_r i_{qr}, \tag{19}$$

$$v_{qr} = r_r i_{qr} + \sigma L_r\frac{di_{qr}}{dt} + \omega_r\sigma L_r i_{dr} + \omega_r\frac{L_m}{L_s}\psi_s. \tag{20}$$

The voltages in $dq$ references can be written as:

$$V_{dr}^* = U_{dr} - \omega_r\sigma L_r i_{qr}, \tag{21}$$

$$V_{qr}^* = U_{qr} + \omega_r\sigma L_r i_{dr} + \omega_r\frac{L_m}{L_s}\psi_s. \tag{22}$$

The vector control of the RSC design is represented in Fig. 5.

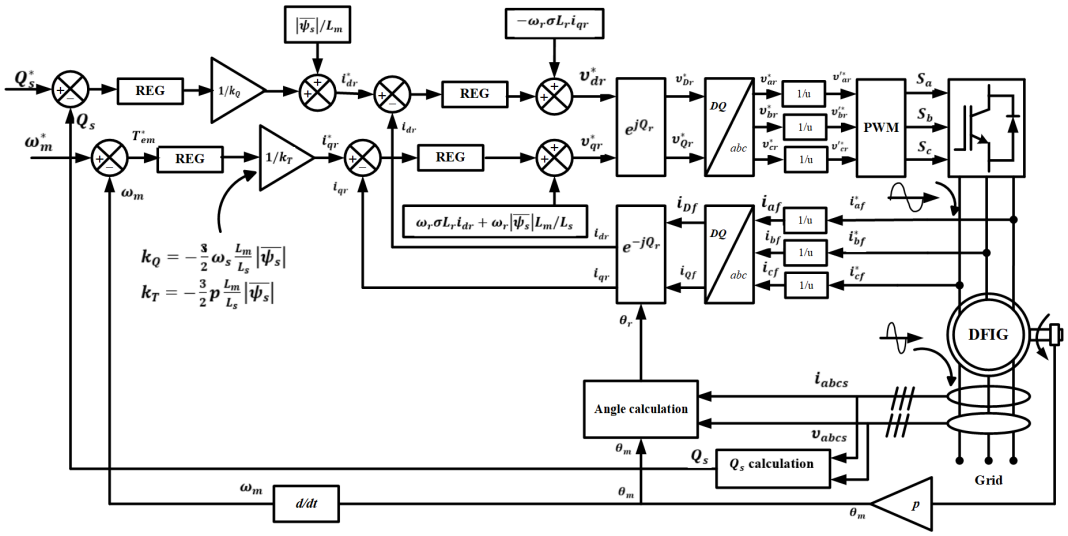


**Fig. 5:** Vector control for the RSC design.

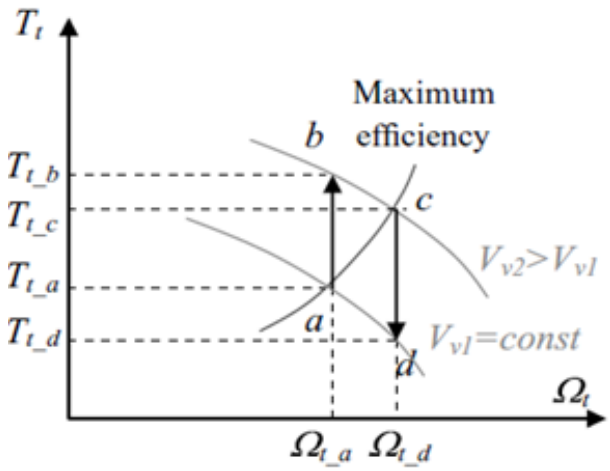


**Fig. 6:** MPPT stability curve [20].

### 3.2. Grid Side Converter Control

The function of GSC is to keep the DC-bus voltage ($V_{bus}$) referred to the stator constant. In our work $V_{bus}$ is given 1150 V. The dynamics of the voltage in the grid side can be represented as follows:

$$v_d = ri_d + L\frac{di_d}{dt} - \omega_e L i_q + v_{d1}, \tag{23}$$

$$v_q = ri_q + L\frac{di_q}{dt} + \omega_e L i_d + v_{q1}. \tag{24}$$

The voltages in $dq$ references may be given as:

$$v_{d1}^* = \omega L i_{qs} + v_{ds}, \tag{25}$$

$$v_{q1}^* = -\omega L i_{ds}. \tag{26}$$

Vector control for the GSC design is indicated in Fig. 7.

## 4. Proposed Control Approach

This section presents two types of control method of DFIG that has been implemented in the system simulations.

### 4.1. MPPT Technique

A MPPT control strategy is significant since it assures a variable speed system, which maximizes power production throughout a particular wind speed. Consider the curve shown in Fig. 6, the variable speed system is operating at a level. Once the value of wind speed changes from $Vv1$ to $Vv2$, then operating point and torque change to b and $T_{t-b}$, respectively. The regulator produces torque that corresponds with the maximum power curve (level $c$), which is less than $T_{t-b}$. Thus, this increases the rotor speed of the turbine until it reaches level $c$ (equilibrium point).

Rotor speed reference at optimum lambda is given by:

$$\omega_{ref}\,(u) = \frac{\lambda_{opt} v}{R}. \tag{27}$$

The electromagnetic torque ($T_{em}$) can be given:

$$T_{em} = \frac{1}{2}\rho\pi R^3 \frac{R^2\Omega^2}{(\lambda_{opt})^2}\frac{(C_p)_{\max}}{\lambda_{opt}}. \tag{28}$$

Simplifying Equation (28) gives:

$$T_{em} = -k_{opt}\Omega^2. \tag{29}$$

Equation (29) leads to Fig. 8

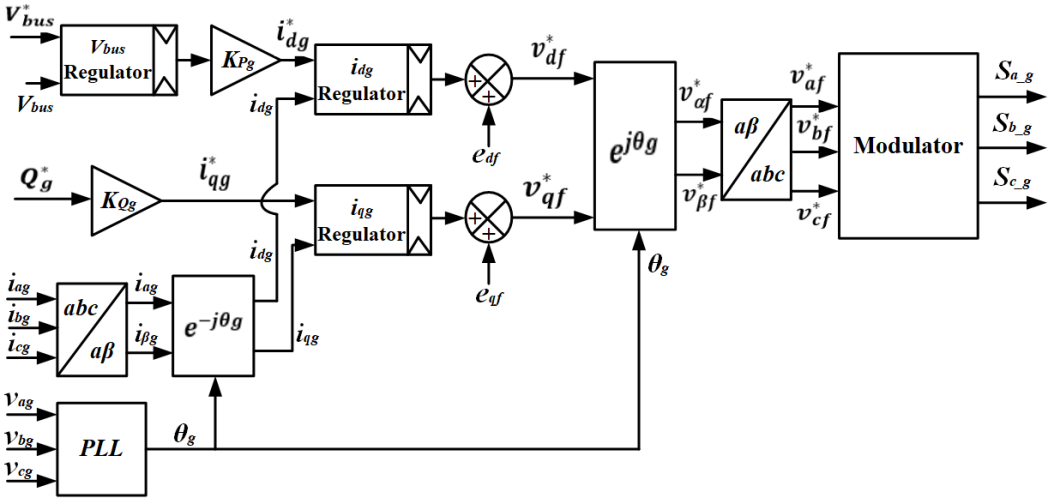


**Fig. 7:** Vector control for the GSC design.

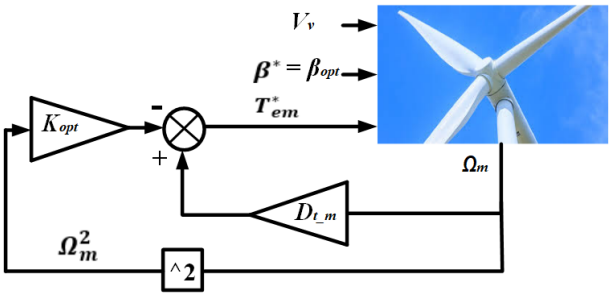


**Fig. 8:** MPPT control strategy.

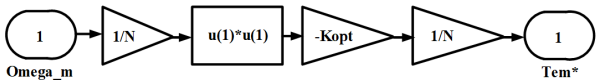


**Fig. 9:** Simulink model of MPPT control strategy.

### 4.2. PI Controller

It is very important to create PI regulators. Fig. 10 illustrates the turbine coefficient as a function of lambda and power curve. Here, the suggested power curve (Fig. 10) is verified by comparing the values of power of the DFIG system with different wind speed.

The specifications of wind turbine system are given in Tab. 2.

## 5. Result and Discussion

In this study, the real parameters of MWT 92/2.4 MW wind turbine of the Mitsubishi have been implemented for simulation study. Hence, the overall system has been verified by MATLAB/Simulink environment. Furthermore, the grid voltage and switching frequency are constant throughout the simulation, i.e., voltage is

**Tab. 2:** Values of $z_o$ for various landscape type [24].

| | |
|---|---|
| Nominal power (Ps) | 2.4 MW |
| The Rated torque (Tem) | 12732 Nm. |
| Rotor speed I (n) | 157.08 rad/sec |
| Rotor speed II (n) | 188.49 rad/sec |
| | |
| DC-bus voltage | 1150 V |
| Bus capacitance | 0.08 F |
| | |
| Stator resistance (Rs) | 0.0026 Ω |
| Stator inductance (Ls) | 0.002587 H |
| | |
| Rotor resistance (Rr) | 0.0261 Ω |
| Rotor inductance (Lr) | 0.002587 H |

690 V, and frequency is 4000 Hz. Fig. 11 represents the Simulink model of PI controller.

The DFIG system operation is first conducted using typical PI and MPPT controller, then the comparison of the overall system with the two controllers is performed in terms of settling time in Tab. 3. For instance, the reference speed is set to be 1500 rpm (157.08 rad/sec) the simulation of PI controller started with 90% of reference speed (see Fig. 12), the rotor speed is operating as sub-synchronous (motor mode) up to 4 sec, then at 4 sec the operation is changed to synchronous mode (100% of the reference speed), later at the simulation time ($t_s = 6s$) the operation is changed to hyper-synchronous (generator mode) with the same rated torque. Similarly, the electromagnetic torque is controlled according to the synchronous speed. Fig. 14 presents the quadrature rotor current $i_{qr}$ that is changing according to the electromagnetic torque, because torque is proportional to the quadrature rotor current.

One DFIG system is found to be sensitive to the grid disturbances. Normally, the rotor side of DFIG is connected to the grid via converter. Thus, when a

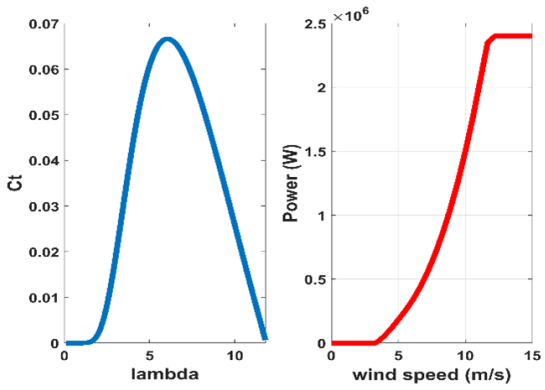


**Fig. 10:** Torque coefficient versus lambda and power curve.

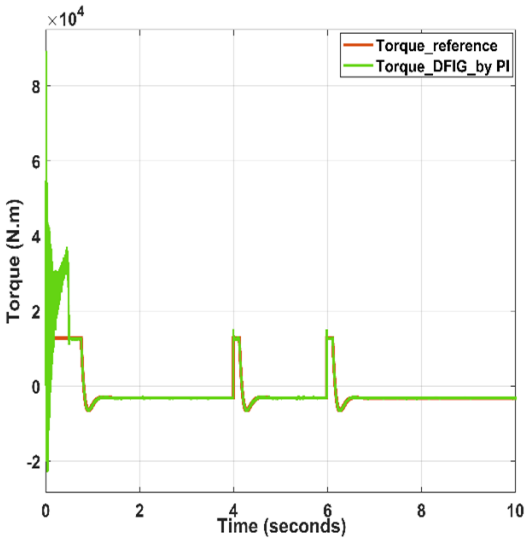


**Fig. 13:** Electromagnetic torque of DFIG.

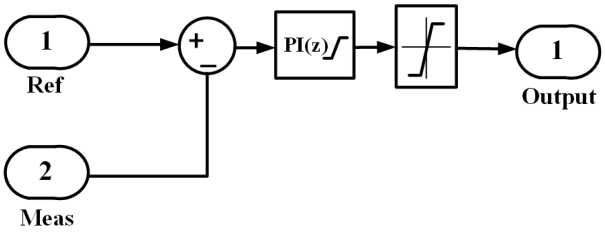


**Fig. 11:** Simulink model of MPPT control strategy.

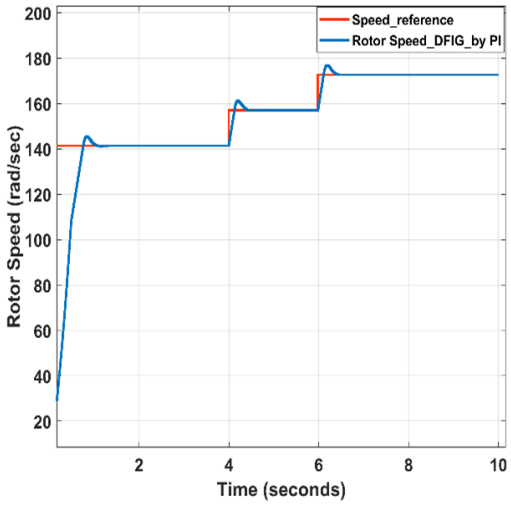


**Fig. 12:** Rotor speed of DFIG.

grid fault occurs the converter will be damaged. However, this can be addressed through the use of some hardware protections such as crowbar protection and DC choppers. One of the mainy, advantage of DFIG system integrated with the wind turbines is that the stator voltage and frequency remain constant, regardless of how the speed of the wind blows on the turbine rotor. At this point, the wind speed profile is set to be 8.5 m/s. Furthermore, the wind speed model is designed by adding four constituents such as constant, turbulence, ramp, and gust constituents. The gust constituents are used to describe the unusual sudden changes in wind speed. Equation (4) leads to the wind speed profile represented in Fig. 15. Taking the RSC into consideration, the rotor speed is set to 136.5 rad/sec at steady state and the wind speed is modified to 11.5 m/s at 4 seconds, As a result, the rotor speed increased to 196.4 rad/sec, as shown in Fig. 16. Similarly, Fig. 17 presents the electromagnetic torque at wind speeds of 8.5 m/s and 11.5 m/s, resulting -5500 Nm and -11500 Nm of generated torque, respectively. Accordingly, the generated power is modified to -0.75 MW and -2.25 MW, respectively.

The generated torque and power are negative because the machine is operating as a generator convention. Fig. 18 represents the quadrature rotor current ($i_q$), and Fig. 19 shows the stator active power which modifies according to $i_q$. Fig. 20 indicates the direct rotor current $i_dr$, which is set to 850 A at 6 seconds and reactive stator power is controlling and modifying according to $i_dr$ as shown in Fig. 21.

In GSC, the DC-bus voltage is set to be 1150 V, as shown in Fig. 22, DC bus voltage is maintaining constant at 1150 V at the steady-state with the change in torque. Fig. 23 represents grid reactive reference

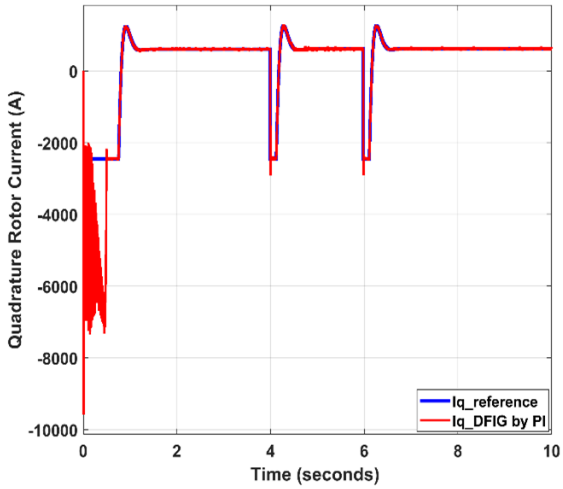


**Fig. 14:** Quadrature rotor current of DFIG.

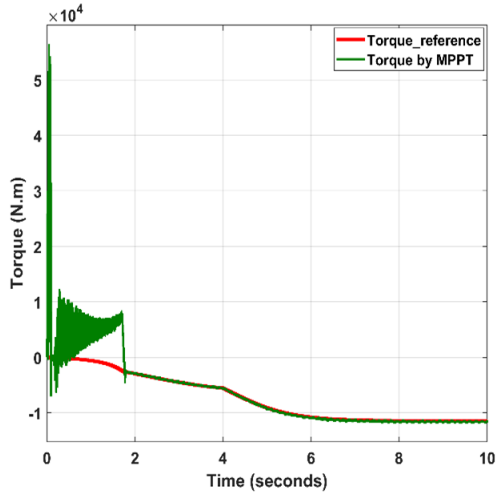


**Fig. 17:** Generated torque of DFIG based wind turbine.

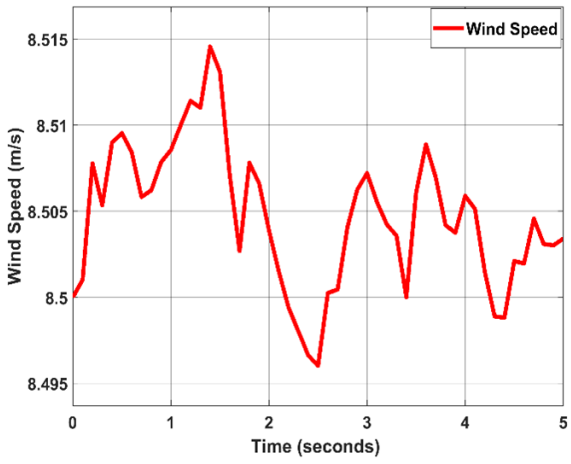


**Fig. 15:** Wind speed profile at 8.5 m/s.

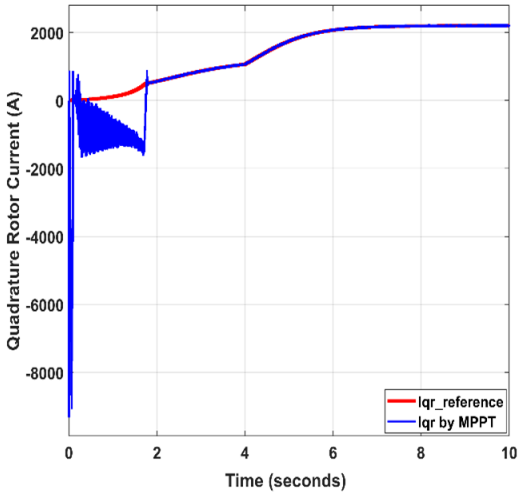


**Fig. 18:** Quadrature rotor current.

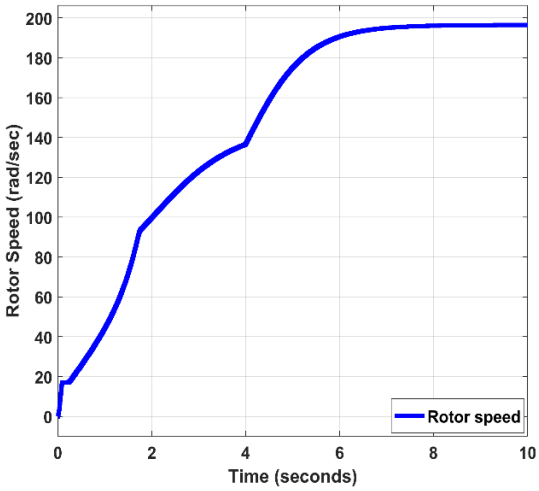


**Fig. 16:** Rotor speed at different wind speed.

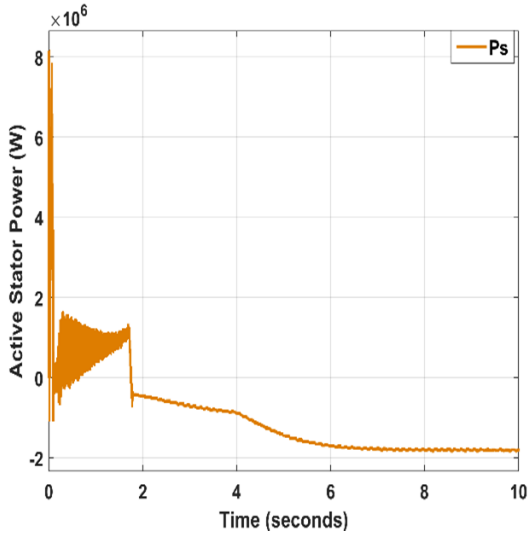


**Fig. 19:** Active stator power.

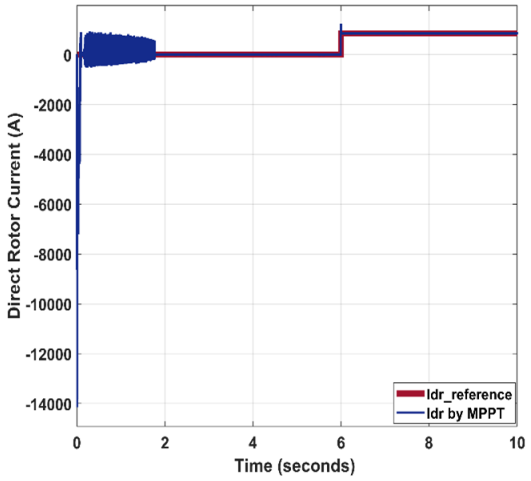


**Fig. 20:** Direct rotor current.

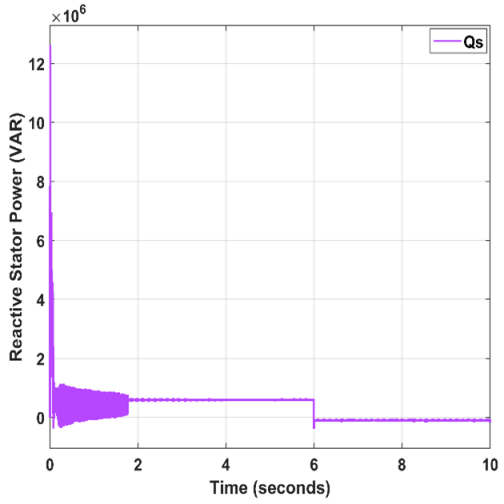


**Fig. 21:** Stator reactive power.

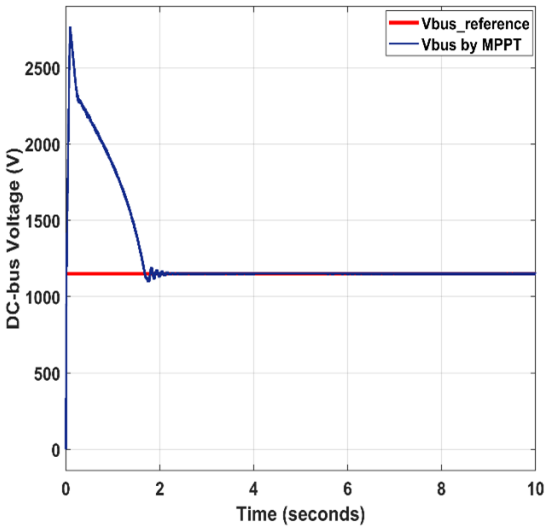


**Fig. 22:** Reperesentation of the DC-bus voltage.

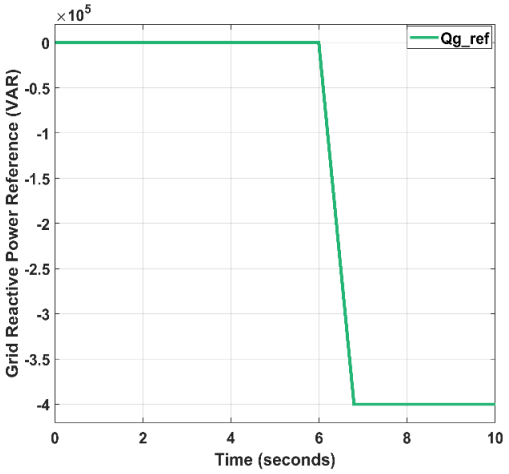


**Fig. 23:** Represents the grid reactive power reference.

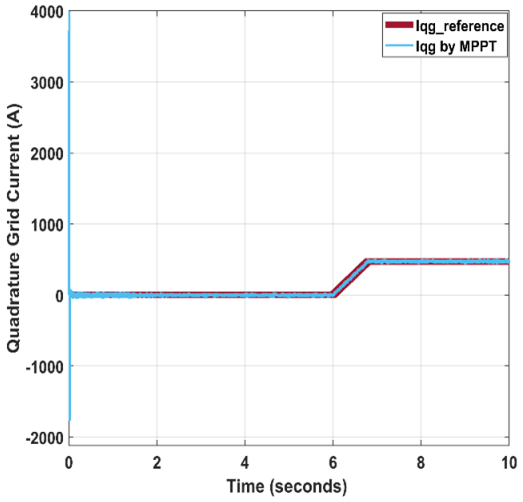


**Fig. 24:** Performance of the quadrature grid current.

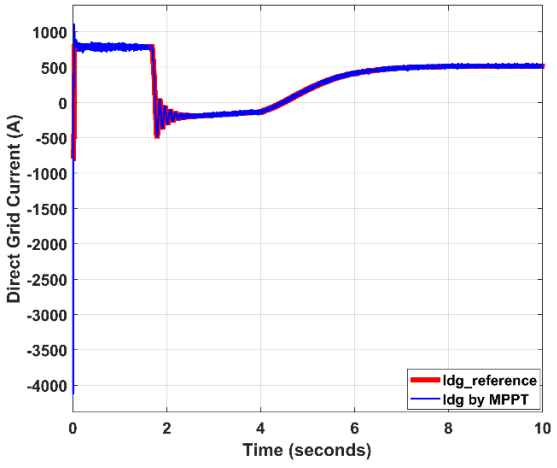


**Fig. 25:** Direct grid current.

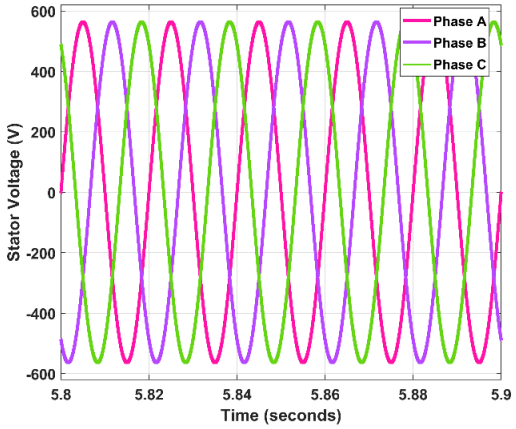


**Fig. 26:** Three phase stator voltage.

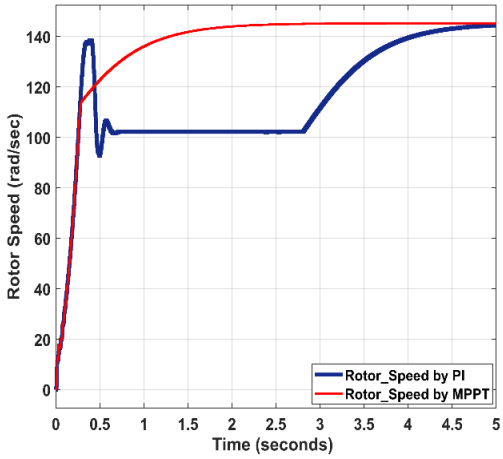


**Fig. 27:** Steady state response of rotor speed with MPPT and PI controller at 8.5 m/s.

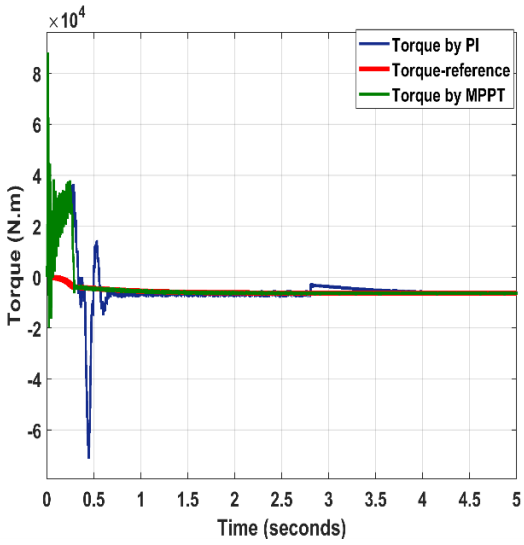


**Fig. 28:** Steady state response of torque with MPPT and PI controller at 8.5 m/s.

($Q_{g\_ref}$), which, for instance, is set to be zero up to $t_s = 6$s. and changed to -400 kVAR and is maintaining and tracking the desired value. Furthermore, $Q_{g\_ref}$ can be changed according to the desired grid code. In Fig. 24, the quadrature grid current is changing according to the change in $Q_{g\_ref}$. Fig. 25 and Fig. 26 represent direct grid current ($i_{dg}$) and three phase stator voltages, respectively. As shown from the rotor speed (by MPPT) in Fig. 16, as the wind speed increases, torque and generated power also increases. However, in this work the wind speed doesn't go beyond 11.8 m/s. For instance, in case it exceeds that value, the pitch controller will take place to limit the maximum extracted power. Even though, pitch controller is not implemented, instead parameters of Mitsubishi MWT 92 have been carried out in MATLAB (see Fig. 10). Thus, the result shown in Fig. 27, Fig. 28, Fig. 29 and Fig. 30 has been compared and verified with Fig. 10.

**Tab. 3:** Summary of the best results from three study cases by running Simulation data inspector.

| Wind speed | Settling Time (%5) | | | |
|---|---|---|---|---|
| | DFIG magnitudes | PI controller | MPPT control | Unit |
| 8.5 m/s | Rotor speed | 4.5 | 1.4 | second |
| | Torque | 4.9 | 2.1 | second |
| | Iq | 5.1 | 1.8 | second |
| | Id | 1.1 | 0.891 | second |
| 9.5 m/s | Rotor speed | 3.71 | 1.35 | second |
| | Torque | 3.914 | 1.94 | second |
| | Iq | 4.476 | 1.76 | second |
| | Id | 1.03 | 0.81 | second |
| 11.8 m/s | Rotor speed | 3.218 | 1.33 | second |
| | Torque | 3.64 | 1.7 | second |
| | Iq | 4.1 | 1.613 | second |
| | Id | 0.91 | 0.705 | second |

In this study, the rotor speed response, generated torque, quadrature rotor current and direct rotor current were mainly investigated. In the literature, optimum control of a DFIG system using differential evolusionary strategy are presented to improve the performances of DFIG systems during perturbation [29] and [31]. Accordingly, by using fuzzy-PI controller in [15] and [30], the settling time and the value of peak overshoot have reduced, and variations are damped down faster when compared with typical PI controller. Besides, the transient response given by fuzzy-PI controller has also proved to be better than typical PI controller. Compared to the aforementioned literature with this work, as illustrated in above results (Fig. 27, Fig. 28, Fig. 29 and Fig. 30), it can be seen that there is higher overshoot/undershoot in the PI-controller representation. Further, this higher overshoot and undershoot can be ruduced by tunning the PI-gains and current loops until the desired values are

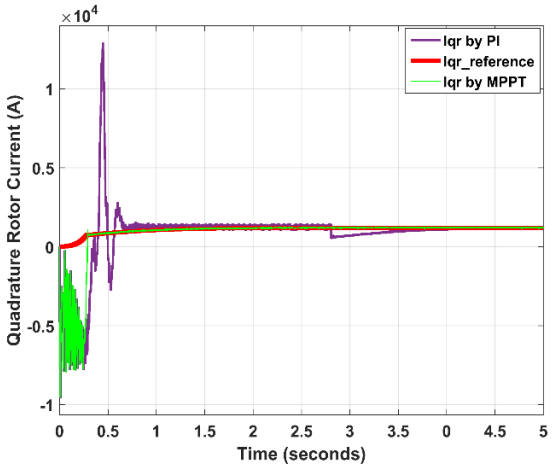


**Fig. 29:** Steady state response of quadrature rotor current with MPPT and PI controller at 8.5 m/s.

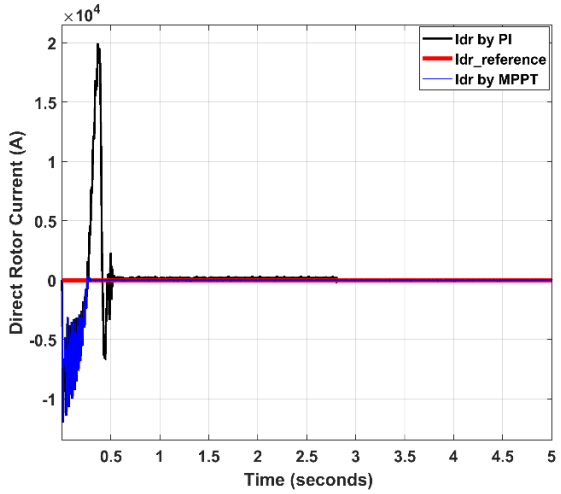


**Fig. 30:** Steady state response of direct rotor current with MPPT and PI controller at 8.5 m/s.

obtained. Meanwhile, the performance of DFIG based wind turbine with the MPPT control improves in terms of settling time as given in Tab. 3. Moreover, it can be observed that the MPPT control has less perturbations and provides strong robustness and reaches the steady state faster with variable parameters. Additionally, active power of the DFIG system matches with the power curve shown in Fig. 10.

## 6. Conclusion

The VC approach has been designed to control the rotor and grid sides of the DFIG system independently. This control strategy reduces harmonic distortion and produces fewer power ripples. The overall system consists of two cases. In Case I, PI controller is applied to the rotor side of DFIG system. Hence, the rotational speed is operating from sub-synchronous to hyper-synchronous mode with a constant input torque. Therefore, a constant rotor speed and constant electromagnetic torque are obtained for a constant reference speed. In case II, MPPT closed loop strategy has been considered. In this strategy, constant rotor speed and generated torque are obtained for a variable wind speed, as a result, the generated power is obtained, and confirmed by comparing it with the extracted power (Fig. 10). Further, the rotor side is able to control the stator's active and reactive power. On the other hand, the grid side controls grid reactive references, which can be controlled according to the grid codes. The grid side is also used to keep the DC bus voltage constant. Thus, PI controllers are effective for fast tracking of current references, and the current loops have been tuned until the desired value is obtained. On the other hand, MPPT control has fewer perturbations, provides strong robustness, and reaches a steady state faster with variable parameters. From the results, it is clearly obvious that the designed MPPT is efficient, reliable, and gives better performance than PI controller.

In the future, the researchers can focus on designing the pitch controller to achieve good performance at much higher wind speeds.

## Author Contributions

S.A.Y. has proposed the modelling and simulation using MATLAB/Simulink 2019a Version. Z.Y. has guided system parameter selection and also supervisor of the overall work. S.A.Y., Z.Y., A.H. and O.T. contributed to writing the manuscript.

## References

[1] BENKAHLA, M., R. TALEB, and Z. BOUDJEMA. Comparative Study of Robust Control Strategies for a Dfig-Based Wind Turbine. *Int. J. Adv. Comput. Sci. Appl.* 2016, vol. 7, iss. 2, pp. 455–462. ISSN 2156-5570. DOI: 10.14569/ijacsa.2016.070261.

[2] JAIN, B., S. JAIN, and R. K. NEMA. Control strategies of grid interfaced wind energy conversion system: An overview. *Renew. Sustain. Energy Rev.* 2015, vol. 47, pp. 983–996. ISSN 1364-0321. DOI: 10.1016/j.rser.2015.03.063.

[3] JENA, D. and S. RAJENDRAN. A review of estimation of effective wind speed based control of wind turbines. *Renew. Sustain. Energy Rev.*

2015, vol. 43, pp. 1046–1062. ISSN 13640321. DOI: 10.1016/j.rser.2014.11.088.

[4] PATI, S. and S. SAMANTRAY. Decoupled control of active and reactive power in a DFIG based wind energy conversion system with conventional P-I controllers. In: *Int. Conf. Circuits, Power Comput. Technol. ICCPCT*. 2014, pp. 898–903. ISSN 978-1-4799-2397-7. DOI: 10.1109/ICCPCT.2014.7054793.

[5] OUYANG, J., T. TANG, J. YAO, and M. LI. Active voltage control for DFIG-based wind farm integrated power system by coordinating active and reactive powers under wind speed variations. *IEEE Trans. Energy Convers.* 2019, vol. 34, iss. 3, pp. 1504–1511. ISSN 0885-8969. DOI: 10.1109/TEC.2019.2905673.

[6] KERROUCHE, K., A. MEZOUAR, and K. BELGACEM. Decoupled control of doubly fed induction generator by vector control for wind energy conversion system. *Energy Procedia*. 2013, vol. 42, pp. 239–248. ISSN 1876-6102. DOI: 10.1016/j.egypro.2013.11.024.

[7] GHOUDELBOURK, S., D. DIB, and A. OMEIRI. Decoupled control of active and reactive power of a wind turbine based on DFIG and matrix converter. *Energy Syst.* 2016, vol. 7, iss. 3, pp. 483–497. ISSN 1868-3967. DOI: 10.1007/s12667-015-0177-1.

[8] AYDIN, E., A. POLAT, and L. T. ERGENE. Vector control of DFIG in wind power applications. In: *IEEE Int. Conf. Renew. Energy Res. Appl. ICRERA*. Birmingham, IEEE, 2016, vol. 5, iss. 1, pp. 478–483. ISSN 978-1-5090-3388-1. DOI: 10.1109/ICRERA.2016.7884383.

[9] JABR, H. M., D. LU, and N. C. KAR. Design and implementation of neuro-fuzzy vector control for wind-driven doubly-fed induction generator. *IEEE Trans. Sustain. Energy*. 2011, vol. 2, iss. 4, pp. 404–413. ISSN 1949-3029. DOI: 10.1109/TSTE.2011.2160374.

[10] LI, S., T. A. HASKEW, K. A. WILLIAMS, and R. P. SWATLOSKI. Control of DFIG wind turbine with direct-current vector control configuration. *IEEE Trans. Sustain. Energy*. 2012, vol. 3, iss. 1, pp. 1–11. ISSN 1949-3029. DOI: 10.1109/TSTE.2011.2167001.

[11] WANG, T., L. DING, S. YIN, J. JIANG, F. CHENG, and J. SI. A new control strategy of DFIG-based wind farms for power system frequency regulation. In: *IEEE PES Asia-Pacific Power and Energy Engineering Conference (APPEEC)*. IEEE, 2015, vol. 3, pp. 1–5. ISSN 978-1-4673-8132-1. DOI: 10.1109/APPEEC.2015.7380877.

[12] HUGHES, F. M., O. ANAYA-LARA, N. JENKINS, and G. STRBAC. Control of DFIG-based wind generation for power network support. *IEEE Trans. Power Syst.* 2005, vol. 20, iss. 4, pp. 1958–1966. ISSN 0885-8950. DOI: 10.1109/TPWRS.2005.857275.

[13] FDAILI, M., A. ESSADKI, and T. NASSER. Comparative analysis between robust SMC & conventional PI controllers used in WECS based on DFIG. *Int. J. Renew. Energy Res.* 2017, vol. 7, iss. 4, pp. 2152–2161. ISSN 1309-0127 DOI: 10.20508/ijrer.v7i4.6441.g7267.

[14] EL AZZAOUI. M. and H. MAHMOUDI. Fuzzy-PI control of a doubly fed induction generator-based wind power system. *Int. J. Autom. Control.* 2017, vol. 11, iss. 1, pp. 54–66. ISSN 1740-7516. DOI: 10.1504/IJAAC.2017.080819.

[15] HAMANE, B., M. BENGHANEM, A. M. BOUZID, A. BELABBES, M. BOUHAMIDA, and A. DRAOU. Control for variable speed wind turbine driving a doubly fed induction generator using fuzzy-PI control. *Energy Procedia*. 2012, vol. 18, pp. 476–485. ISSN 1876-6102. DOI: 10.1016/j.egypro.2012.05.059.

[16] ZHU, R., Z. CHEN, Y. TANG, F. DENG, and X. WU. Dual-loop control strategy for DFIG-based wind turbines under grid voltage disturbances. *IEEE Trans. Power Electron.* 2016, vol. 31, iss. 3, pp. 2239–2253. ISSN 0885-8993. DOI: 10.1109/TPEL.2015.2442520.

[17] TREMBLAY, E., S. ATAYDE, and A. CHANDRA. Comparative study of control strategies for the doubly fed induction generator in wind energy conversion systems: A DSP-based implementation approach. *IEEE Trans. Sustain. Energy*. 2011, vol. 2, iss. 3, pp. 288–299. ISSN 1949-3029. DOI: 10.1109/TSTE.2011.2113381.

[18] NIAN, H. and X. YI. Coordinated control strategy for doubly-fed induction generator with DC connection topology. *IET Renew. Power Gener.* 2015, vol. 9, iss. 7, pp. 747–756. ISSN 1752-1416. DOI: 10.1049/iet-rpg.2014.0347.

[19] WU, Y. K. and W. H. YANG. Different Control Strategies on the Rotor Side Converter in DFIG-based Wind Turbines. *Energy Procedia*. 2016, vol. 100, pp. 551–555. ISSN 1876-6102. DOI: 10.1016/j.egypro.2016.10.217.

[20] ABAD, G., J. LÓPEZ, M. A. RODRÍGUEZ, L. MARROYO, and G. IWANSKI. *Doubly Fed Induction Machine*. Hoboken, NJ, USA: John Wiley & Sons, Inc., 2011. ISBN 9781118104965.

[21] YAICHI, I., A. SEMMAH, and P. WIRA. Direct Power Control of a Wind Turbine Based on Doubly Fed Induction Generator. *Eur. J. Electr. Eng.* 2019, vol. 21, iss. 5, pp. 457–464. ISSN 2103-3641. DOI: 10.18280/ejee.210508.

[22] IBRAHIM, A. Vector control of current regulated inverter connected to grid for wind energy applications. *Int. J. Renew. Energy Technol.* 2009, vol. 1, iss. 1, p. 17. ISSN 1757-3971. DOI: 10.1504/IJRET.2009.024728.

[23] KUMHAR, A. R. Vector Control Strategy to Control Active and Reactive Power of Doubly Fed Induction Generator Based Wind Energy Conversion System. In: *2018 2nd International Conference on Trends in Electronics and Informatics (ICOEI)*. 2018, pp. 1–9. ISBN 978-1-5386-3570-4. DOI: 10.1109/ICOEI.2018.8553761.

[24] JUNYENT-FERRÉ, A., O. GOMIS-BELLMUNT, A. SUMPER, M. SALA, and M. MATA. Modeling and control of the doubly fed induction generator wind turbine. *Simul. Model. Pract. Theory.* 2010, vol. 18, iss. 9, pp. 1365–1381. ISSN 1569-190X. DOI: 10.1016/j.simpat.2010.05.018.

[25] AKHMATOV, V., A. H. NIELSEN, J. K. PEDERSEN, and O. NYMANN. Variable-speed wind turbines with multi-pole synchronous permanent magnet generators. Part I: Modelling in dynamic simulation tools. *Wind Eng.* 2003, vol. 27, iss. 6, pp. 531–548. ISSN 0309-524X. DOI: 10.1260/030952403773617490.

[26] MICHAS, M. Control of Turbine-Based Energy Conversion Systems. *PhD Thesis*, 2018, vol. 2, pp. 1–156. [Online]. Available at: `https://orca.cardiff.ac.uk/id/eprint/117586`.

[27] YANG, B., L. JIANG, L. WANG, W. YAO, and Q. H. WU. Nonlinear maximum power point tracking control and modal analysis of DFIG based wind turbine. *Int. J. Electr. Power Energy Syst.* 2016, vol. 74, pp. 429–436. ISSN 0142-0615. DOI: 10.1016/j.ijepes.2015.07.036.

[28] LAMNADI, M., M. TRIHI, B. BOSSOUFI, and A. BOULEZHAR. Modeling and control of a doubly-fed induction generator for wind turbine-generator systems. *Int. J. Power Electron. Drive Syst.* 2016, vol. 7, iss. 3, pp. 982–995. ISSN 20888694. DOI: 10.11591/ijpeds.v7.i3.pp982-995.

[29] SURYOATMOJO, H., A. M. B. ZAKARIYA, S. ANAM, A. MUSTHOFA, and I. ROBANDI. Optimal controller for doubly fed induction generator (DFIG) using Differential Evolutionary Algorithm (DE). In: *2015 International Seminar on Intelligent Technology and Its Applications (ISITIA)*. 2015, pp. 159–164. ISBN 978-1-4799-7710-9. DOI: 10.1109/ISITIA.2015.7219972.

[30] AL ZABIN. O. and A. ISMAEL. Rotor Current Control Design for DFIG-based Wind Turbine Using PI, FLC and Fuzzy PI Controllers. In: *2019 International Conference on Electrical and Computing Technologies and Applications (ICECTA)*. 2019, pp. 1–6. ISBN 978-1-7281-5532-6. DOI: 10.1109/ICECTA48151.2019.8959530.

[31] ABDİ YONİS. S and Z. YUSUPOV. Dynamic Analysis of Current Loops Behavior in a Wind Turbine Based Doubly-fed Induction Generator. *Eur. J. Sci. Technol.* 2022, iss. 34, pp. 415–420. ISSN 2148-2683, DOI: 10.31590/ejosat.1082326.

# About Authors

**Samatar ABDI YONIS** (Corresponding Author) was born in Djibouti city, Djibouti. He received his B.Sc degree in electrical and computer engineering from Haramaya University and M.Sc in electrical and electronics from Karabuk university in 2018 and 2022, respectively. He is now pursuing toward PhD in electrical and electronics engineering in Karabuk university, Turkiye. His research of interests include power system, renewable energy and control theory.

**Ziyodulla YUSUPOV** received the B.S. & M.S. degree in Electrical-Electronics from the Tashkent State Technical University, Uzbekistan and Ph.D. degree in Electrical-Electronics from the Institute of Power Engineering & Automation of Uzbekistan Academy of Sciences, Uzbekistan, in 1993 and 2010, respectively. Dr. Yusupov is currently a Professor in the Department of Electrical-Electronics Engineering at Karabuk University (Karabuk/ Turkiye). He has over 40 publications, including journal papers, conference papers, and book chapters in the areas of electric drive systems, control systems, multi-agent systems, Smart Grid, and Microgrid. His research interests include control and optimization of microgrid systems, multi-agent systems, and Smart Grids.

**Adib HABBAL** is a Professor (Associate) of Computer Engineering and Founding head of the Innovative Networked Systems (INETs) Research Group at Karabuk University, Turkiye. Before joining Karabuk University in 2019, he was a senior lecturer at Universiti Utara Malaysia (ten years). Dr. Habbal received his Ph.D. degree in Computer Science (specializing in Networked Computing) from Universiti Utara Malaysia. Dr. Habbal has received a number of recognitions from Universiti Utara Malaysia (UUM)

for his outstanding educational and research activities including the Excellent Service Award (2010), Best Research Award (2014), Prolific Writer Award (2016) and many others. He has been the recipient of Internet Society Fellowship to the Internet Engineering Task Force (IETF), an IEEE Malaysia Section Best Volunteer Award, and an Asia-Pacific Advanced Network (APAN) Fellowship. Dr. Habbal is a senior member of the Institute of Electrical and Electronic Engineers (IEEE). Dr. Habbal's research projects have been funded by several organizations, including IEEE R10, IEEE Malaysia Section, Internet society, Malaysian Ministry of Higher Education, Universiti Utara Malaysia and others. He has over 100 publications in journals and conference proceedings in the areas of Future Internet, and performance evaluation. His research interests include Future Internet protocols and architecture, Next Generation Mobile Networks, as well as Blockchain Technology and Digital Trust.

**Olimjon TOIROV** received the B.E. and the M.E. degree in electrical engineering from the Bukhara Institute of Food and Light Industry Technology, Bukhara, Uzbekistan, in 2004 and 2006, respectively. He received his Ph.D. degree in energy systems and complexes from the Institute of Power Engineering and Automatics of the Academy of Sciences of the Republic of Uzbekistan, Tashkent, in 2012, and the DSc degree in energy systems and complexes from the Tashkent State Technical University, Tashkent, Uzbekistan, in 2018. Currently, he is the head of the department of Electrical Machines at the Tashkent State Technical University. He is a member of the Scientific Council for the award of scientific degrees of Doctor of Science No. DSc.03/10.12.2019. T.03.03 at the Tashkent State Technical University. He has published over 150 papers in journals and conference proceedings, 8 methodical manuals, 4 textbooks, 5 training manuals and 1 monograph, actively participated in the implementation of 10 fundamental-practical scientific projects.